4445

Spatial Homogeneity of Air in a Mushroom Tunnel: Single vs. Boost Duct Air Distribution Systems

David P. Martin **John V. Ringwood, Ph.D.** **James J. Grant**

ABSTRACT

Air can become stratified in a standard mushroom tunnel using a single-duct air distribution system. Stratification can be overcome by increased air circulation, such as the addition of a secondary air distribution duct, i.e., a boost duct air distribution system. To compare the performance of both systems, this study measured the spatial variation in climate for both systems. Air temperature, humidity, and speed were monitored at representative locations in one-half of the tunnel, as bilateral symmetry in air distribution has been previously observed. The experiments, including replicates, were conducted for both full recirculation and full fresh air. A vertical mean air temperature difference of 0.22°C was observed for the boost air distribution system and 2.22°C for the single air distribution system. No significant longitudinal difference was observed for either system. The lower vertical air temperature difference of the boost system shows its superior mixing performance.

INTRODUCTION

Spatial variation in mushroom tunnel climate has a major impact on the choice of climate model form. If spatial variance is low, there is a case for using a single set of lumped climatic parameters, i.e., air temperature, humidity, and contamination, which are indicative of the state of the air in the tunnel as a whole. Conversely, if spatial variance is high, then multiple sets of spatially distributed climatic parameters are a more appropriate model form.

If the air in a tunnel is well mixed, there is justification for a perfect mixing assumption, which is a necessary condition for the development of a lumped parameter climate model. This study is a precursor to the development of a climate model for Irish mushroom tunnels. By determining how well mixed the air is, selection of model form is facilitated.

The means of mixing the air in a mushroom tunnel is by fan-powered mechanical ventilation through a polyethylene air distribution duct. The air jets leaving the D-shaped vents of the duct entrain tunnel air and instigate mixing between the incoming ventilation air and the tunnel air. Therefore, control of these jets is a means of controlling mixing, and the question then arises as to what is an appropriate jet trajectory control measure.

Objectives

The objectives of this study were

1. to compare the mixing performance of single and boost duct air distribution systems by evaluating the vertical and longitudinal variation of climate in a standard tunnel and
2. to identify a variable for control of the air distribution system.

In relation to objective 1, previous measurements (Grant 1995a; Martin et al. 1997) have shown that the air is not always well mixed in single-duct systems, with an ensuing local variation in climate, particularly in the vertical dimension, i.e., increasing z, where air temperature can rise by nearly 2 K/m (3.6°F/ft). Spatial variation in thermal energy, i.e., enthalpy, can be calculated from air temperature and humidity. Spatial variation in kinetic energy can be calculated from air mass and airspeed. Finally, spatial variation in mass can be calculated from air temperature and humidity. Using the standard ventilation assumption that one marker can be used as an indicator for a group of correlated gases, spatial variation in contaminant levels, e.g., carbon dioxide, can be calculated from measured variations in water vapor.

David Martin is a researcher and **John Ringwood** is a professor in the Department of Electronic Engineering, National University of Ireland, Maynooth, Ireland. **Jim Grant** is a researcher at the Kinsealy Research Centre, Teagasc, Dublin.

Air Distribution Systems

Evaporation is a key parameter for good mushroom growth and it can be manipulated by control of the drying power of the air. Drying power is taken as the product of water vapor deficit and airspeed. Stratification of tunnel air is currently an obstacle to controlling the drying power of the air at the crop level because of its effect on airspeed.

Irish mushroom tunnels generally have an air conditioner located at one end of a tunnel, feeding a single longitudinal central overhead polyethylene air distribution duct. Single-duct air distribution systems are installed in most Irish mushroom tunnels. The fan in such systems cannot deliver the required momentum increase with full heating, and tunnel air can become stratified, i.e., when primary duct air jets operate in nonisothermal conditions (Grant 1995b). A secondary "boost" duct and fan air distribution system can increase airflow and eliminate stratification. The layout and a photo of a boost duct system that can be retrofitted into existing single-duct tunnels are shown in Figure 1.

Operation of the heater changes the thermal buoyancy of the distributed air; consequently, the air in the tunnel can become stratified, as shown in Figure 2. Note that air stratification in mushroom tunnels and the boost duct solution is discussed more fully by Grant (1999). Figure 3 shows one-half of each of the symmetrical lateral airflows for both single (left-hand side) and boost (right-hand side) duct air distribution systems. To quantify the increased performance of a boost duct system over a single-duct system, two sets of measurements were made, one using both ducts, i.e., a boost duct system, and one using the upper primary duct only, i.e., a single-duct system.

Grant (1995a, 1995b) described thermal and airspeed variations in a single-duct mushroom tunnel but did not discuss the boost duct system. Although previous studies have been conducted for similarly shaped naturally ventilated buildings, e.g., plastic greenhouse tunnels (Wang et al. 1999), the authors have not located any study that quantified the spatial variation of climate in a mechanically ventilated boost

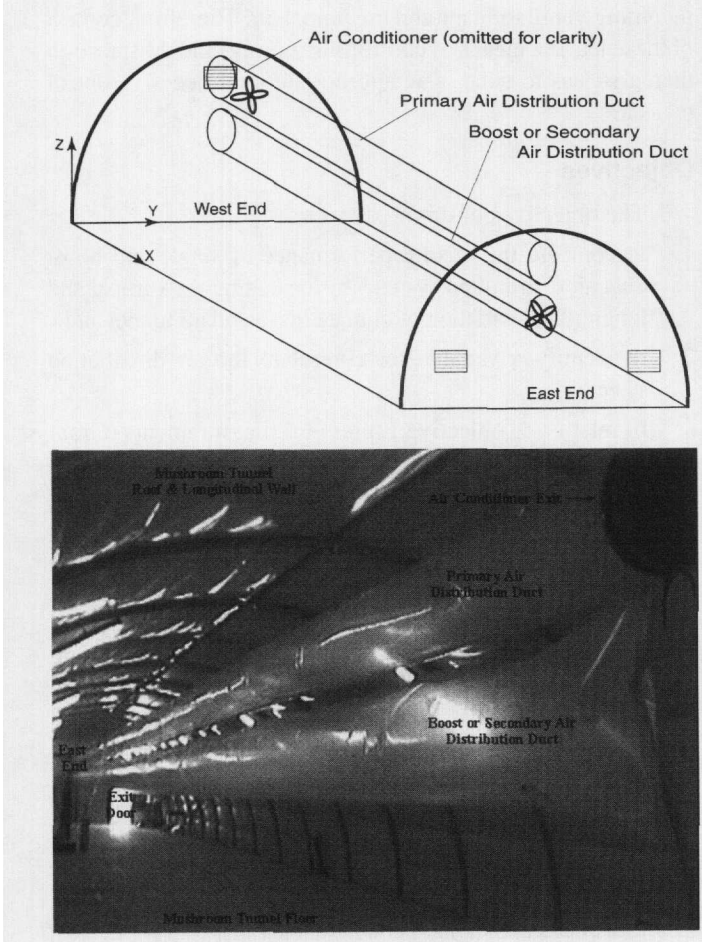

Figure 1 *Layout and photo of a boost duct air distribution system in an Irish mushroom tunnel.*

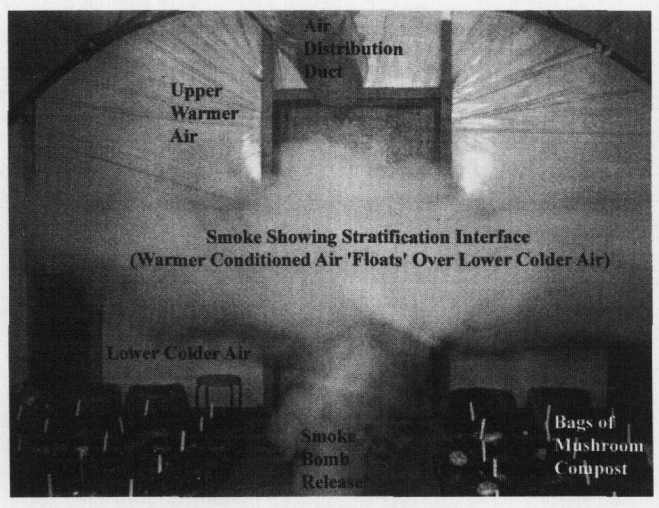

Figure 2 *Smoke bomb photo (Murray 1995) of stratification interface between warmer upper air and colder lower air.*

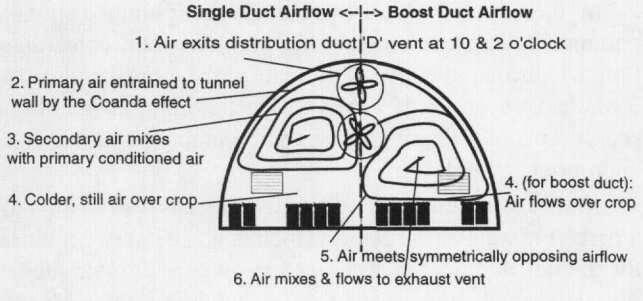

Figure 3 *Based on authors' observations of flow visualization: left-hand side, idealized flow layout for stratified bilateral airflow in an Irish mushroom tunnel; right-hand side, idealized flow layout for boost duct air distribution system in an Irish mushroom tunnel.*

duct mushroom tunnel or one that compared the two air distribution systems.

In relation to objective 2, the Archimedes number (AR) has been used (Randall 1975) as an indicator of the path of an air jet leaving an air delivery duct and entering an air space. Equation 1 shows one form based on the Etheridge and Sandberg (1996) definition for the case of a nonisothermal horizontal jet supplied horizontally.

$$AR_0 = g\,\Delta\rho\,\rho_0^{-1}\,A_0^{0.5}\,u_0^{-2} \quad (1)$$

where

AR_0 = Archimedes number at the plane of jet entry,
g = acceleration due to gravity,
$\Delta\rho$ = density difference between jet entry (ρ_0) and the environment,
ρ_0 = jet density at the plane of jet entry,
A_0 = orifice area at the plane of jet entry,
u_0 = jet velocity at the plane of entry.

EXPERIMENTAL SETUP

An empty tunnel at a research center in Dublin with floor dimensions of 33.54 m (110 ft) by 6.7 m (22 ft), of standard construction (FDS 1987), was used in this study. Latitude, longitude, and elevation for the tunnel are 53° 25.22'N, 06° 10.25'W, and 30 m (97.5 ft), respectively. The tunnel was kept empty for the duration of the measurements because a crop could possibly have a local variation in metabolic output with an ensuing local climate variation. Therefore, no uncontrolled source was in the tunnel during the experimental period.

The longitudinal axis of the tunnel was approximately east-west and the lateral axis of the tunnel was approximately north-south. The sensor sites were positioned using an x, y, z coordinate system where the origin, 0, 0, 0, was the concrete surface at the southwest corner of the tunnel. As shown in Figure 1, for these coordinates,

- positive x values were meters (feet) east and negative x values west from the origin,
- positive y values were meters (feet) north and negative y values south from the origin,
- positive z values were meters (feet) up and negative z values down from the concrete surface.

The concrete surface sloped gently downward from west to east to facilitate water runoff, with a vertical drop of 0.3 m (1 ft) in the 33.54 m (110 ft) length of the tunnel.

Experimental Design

Due to a limited supply of loggers and sensors, the issue of resource optimization and the ensuing implications arose. The possibility was considered of measuring climate on as fine a spatial grid as equipment supply would permit, in a series of experiments that successively sampled lateral slices of the air at different longitudinal intervals, or horizontal slices of the air at different vertical levels, or a combination of both slicing mechanisms. This is arguably the configuration for determining the spatial homogeneity of air in the tunnel at the highest resolution. This approach was not used for several reasons:

1. As the experimental site was field based, no control was available over the climate to which the tunnel as a whole was exposed. Hence, control of tunnel climate for two successive slices could not be guaranteed. While this was more relevant to experiments where full fresh air ventilation was used compared to full recirculation, it could not be dismissed in either case. Consequently, the correlation of climate data from each slice would have been quite problematic.
2. Uncertainty in the position of sensors would increase, as they would have to be repeatedly moved and then repositioned.
3. The cost of the experiment (composed of several subexperiments in this scenario) would multiply in proportion to the interval choice used for the sampling grid.
4. While it was climate at the crop (or floor) level that was of most concern, i.e., the horizontal plane, the mixing performance of the two air distribution systems compared was most visible in the vertical plane, and this has been observed to greatly affect what happens at the crop level.

Climate sensors were positioned in three locations in the tunnel for the duration of the study. The measurement locations were chosen using an assumption of bilateral symmetry along the longitudinal axis of the tunnel. Bilateral symmetry was previously observed using smoke for flow visualization. Note that the point of chief interest for climate control was at the crop level, which corresponds to floor level measurement in this study.

West, middle, and east site positions in the tunnel's southern half were chosen as longitudinal and lateral representatives of the airspace. Sensor site positions are given in Table 1. To eliminate boundary layer effects, all internal air sensing positions had a minimum clearance of 0.1 m (0.3 ft) from any adjacent surface. Airspace measurements were made with z, i.e., vertical, coordinates of:

- 2.55 m (8.4 ft)—duct exit level (D),
- 1.75 m (5.7 ft)—upper mid-airspace (U),
- 0.95 m (3.1 ft)—lower mid-airspace (L),
- 0.15 m (0.5 ft)—floor level (F).

Positional accuracy of sensor location was estimated as being approximately 0.1 m (0.3 ft) for lateral and longitudinal axes and approximately 0.01 m (0.03 ft) for the vertical axis. To minimize the uncertainty of sensor location, all sensors remained in the same position throughout the experiment.

At least three experiments (runs) were conducted for each setup, i.e., all combinations of single or boost duct and 100% recirculation, i.e., ventilation damper fully closed or 100% fresh air, i.e., ventilation damper fully open, in an attempt to

TABLE 1
Sensor Positions in Mushroom Tunnel

West site sensors: x = 5.55 m (18.2 ft), y = 1.65 m (5.4 ft), z = D, U, L, or F

Sensor	Channel	Unit	Vertical Position (z)
H101	9	%RH	D
H101	3	°C	D
T101	1	°C	U
T102	2	°C	L
H102	4	°C	F
H102	10	%RH	F
A101	5	cm/s	F
Φ_P	7	Vrms	D
Φ_S	8	Vrms	U
Φ_h	11	L/m	D
Φ_c	12	L/m	D

Middle site sensors: x = 16.55 m (54.3 ft), y = 1.65 m (5.4 ft), z = D, U, L, or F

Sensor	Channel	Unit	Vertical Position (z)
H201	9	%RH	D
H201	3	°C	D
T201	1	°C	U
T202	2	°C	L
H202	4	°C	F
H202	10	%RH	F
A201	5	cm/s	D
A202	6	cm/s	U
A203	7	cm/s	L
A204	8	cm/s	F

East site sensors: x = 27.50 m (90.2 ft), y = 1.65 m (5.4 ft), z = D, U, L, or F

Sensor	Channel	Unit	Vertical Position (z)
H301	9	%RH	D
T303	3	°C	D
T301	1	°C	U
T302	2	°C	L
T304	4	°C	F
H302	10	%RH	F

encompass a range of weather (load) conditions. It was not the objective of this study to include weather conditions in any mixing performance comparison. Instead, the objective was to see if any correlation in spatial variation was a result of different weather conditions, i.e., variation in heat load.

Sensors

A positional constraint arose due to the limited supply of airspeed sensors. A stand of four sensors and a single airspeed sensor were available, which meant that airspeed could only be measured at two longitudinal sample positions in the tunnel. The stand of four airspeed sensors was placed in the tunnel middle and the single airspeed sensor was placed at the west floor level sensor site.

All sensors were numbered to provide traceability. The capacitive polymer humidity sensors used to measure relative humidity (RH) also had an integral thermistor for temperature sensing. The thermal anemometers used to measure airspeed were temperature compensated. Conversion of the voltage output of the anemometers to airspeed was done using a software implementation of a fifth order polynomial, provided by the manufacturer, for the stand of four sensors or multiplication by a constant for the single anemometer. The battery-powered data loggers, used to record sample values, provided the humidity and temperature values directly. The loggers each had the capability to read

- four temperatures,
- two humidities,
- two counts/frequencies,
- four analog signals.

At the west site, two logger count inputs were used for monitoring air conditioner actuators by recording the milliliter (0.00022 gl) pulse output of two flowmeters, one for heater fluid flow (Φ_h) and one for cooler fluid flow (Φ_c). One of the logger analog inputs was used to record the single anemometer voltage output, and two more were used for monitoring of the fan speed control voltages (Φ_P and Φ_S) as measured by true-RMS voltmeters. Air temperature was measured at the D, U, L, and F vertical positions and humidity at the D and F vertical positions.

At the middle site, the four logger analog inputs were used to record the stand of four anemometer voltage outputs at the D, U, L, and F vertical positions. Air temperature was measured at the D, U, L, and F vertical positions and humidity at the D and F vertical positions.

At the east site, the logger was used to record air temperature at the D, U, L, and F vertical positions and humidity at the D and F vertical positions.

Sensor Calibration

The calibration objective was to calibrate all sensors using the highest calibration standard reference available. All

air sensor calibrations are traceable to Danish, U.K., or Irish accredited laboratories through transfer standards.

A new stand of four airspeed sensors was calibrated at the factory, as was the single airspeed sensor, providing traceability to a nationally accredited laboratory. The uncertainty quoted for the stand of four sensors was ±0.02 m/s (±0.07 ft/s) of reading below 0.7 m/s (2.3 ft/s), and for the single sensor it was ±0.01 m (0.03 ft) ±5% of reading for the range 0.05-1.0 m/s (0.16-3.28 ft/s).

Temperature Sensors

Stainless steel encapsulated thermistor temperature sensors, with a resolution of 0.05 K (0.09°F), were used to monitor air temperature. A three-point calibration, at 288.16 K (59.02°F), 293.17 K (68.04°F), and 298.16 K (77.02°F), was performed on two transfer standards, T303 and T304, in an independent metrology laboratory. The maximum difference between the standards and the calibration system was 0.02 K (0.036°F). The metrology temperature calibration system used a 25 Ω precision standard platinum resistance thermometer (SPRT) immersed in a continuously stirred, temperature-controlled water bath. Using a resistance bridge provides 0.1 mK (0.00018°F) resolution with a total calibration system uncertainty of 0.02 K (0.036°F) (Cromwell 1999). The calibration SPRT was itself calibrated against physical references every six weeks and was calibrated on the day of measurement. For the temperature range of interest in this study, the physical references are the triple point of water for 273.16 K (32.0°F) and a Gallium cell for 302.9146 K (85.6°F).

A bias greater than double-quoted accuracy was detected on some of the temperature sensors used, so these were bias compensated against the transfer standard, T303. All sensors were checked for drift after the experiment, and none was detected. On-site bias compensation was achieved by placing all the temperature and humidity sensors in an air distribution duct that provided air at a range of temperatures. The sensors were kept close together to measure the same airflow but splayed apart to ensure that physical contact did not introduce mutual shadowing errors. The mean difference between the reference and each sensor was then determined and used for bias compensation.

Humidity Sensors

All of the sensors used for humidity measurement were calibrated prior to use and checked for drift afterward. The capacitive polymer RH sensors used had a laboratory two-point calibration, using room air and a saturated salt solution of potassium sulphate (K_2SO_4), following the manufacturer's recommended procedure as a guideline. This provides sensors with a quoted accuracy of 3% of reading above 80% RH and 2% of reading below 80% RH. Additionally, the sensors were checked against a U.K. national standard traceable calibration by using a chilled mirror precision hygrometer with a dew-point accuracy of ±0.2 K (0.36°F) and resolution of 0.1% RH. The manufacturer's recommended calibration procedure omitted a discussion on mixing and on sensor to calibration vessel volume ratio.

Mixing was addressed by inserting a mixing fan in the RH calibration vessel, a fermentation tank. The fan was mounted on a machined flange and suspended in mid-vessel. The fan used was a 12 V (dc), 0.08 m (0.26 ft) diameter, 8.8 dm^3/s (2.32 gps) axial flow fan. Thus, the nominal recirculation or turnover rate in the 25 dm^3 (6.6 gl) fermentation vessel was over 1200 volumes per hour. Dilution of the vessel airspace occurred every time a sensor was inserted or withdrawn from the vessel. As sensors had to be withdrawn and inserted into the airspace several times during the long calibration procedure, it was necessary to ensure that the sensor volume was very much smaller than the vessel. The vessel airspace was checked with the precision hygrometer to test for dilution effects. No such dilution effects were detected.

Measurement System Checkout

To detect any discrepancies arising from specific logger-sensor couplings, the three loggers used were "rotated" between sensor sites. This detected a fault in logger number 3, i.e., the integral temperature sensor in the humidity probe malfunctioned with this particular logger. No other fault was detected by the logger rotation.

It was already known from previous experiments that the loggers had a storage fault. This fault inserted a null value at regular intervals instead of a sampled value on a particular logger channel. Substitution of the null value by interpolation between adjacent values was used to overcome this fault.

A check for noise in the measurement system identified two sources of noise, one being electromagnetic interference and the other being a "noisy" humidity signal. The DC voltage output signal of two RMS voltmeters, used to monitor fan control voltages, appeared as a noisy log compared to a steady voltmeter display. Because of their low voltage/power operation, it was a surprise to identify, by selectively powering down different equipment, the source of the noise as the stand of four anemometers. As the function of the fan logs was to identify an unscheduled power outage, the noisy log was adequate.

The noisy humidity signal was identified as holes in the concrete floor that were made for the insertion of soil temperature sensors in a subsequent experiment. During periods when the air is stratified, the floor level air is relatively stagnant and a positive airflow over the floor-level sensors is not guaranteed. During these periods, relatively humid air from adjacent open holes in the concrete could migrate to the sensor and cause a noisy signal. This was particularly evident following a period of rain. Covering the open holes with an impermeable layer of polyethylene removed the noisy profile of this signal.

MEASUREMENT PROCEDURE

The air conditioner was used to provide a climate state for the air in the tunnel that was similar to that during crop growth. The air temperature set point was 291.15 K (64.4°F), +2 K (3.6°F) hysteresis, with humidity uncontrolled. The thermostat sensor used to switch on the heater at 291.15 K (64.4°F) and off at 293.15 K (68°F) was located at approximately 23.0 m (75.5 ft), 2.0 m (6.6 ft), and 1.57 m (5.2 ft). Throughout the experiments, flow in the cooler was set to zero using a closed supply gate valve and the humidifier was powered off.

As spatial analysis is dependent on achieving equilibrium of the climate profile, the air was maximally mixed for a period of ten minutes prior to setting the crop level airflow to the nominal mean airspeed of 0.25 m/s (0.82 ft/s). Both ducts were used for mixing during single-duct experiments with the upper, primary fan set at 0.875 m^3/s (832 142 gph) and the lower, secondary fan set at 1.123 m^3/s (1 067 783 gph). Once the air was well mixed, i.e., close vertical agreement of temperatures, the boost duct was switched off for single-duct experiments.

The steps used in each experiment were as follows:

1. The ventilation damper angle was set for 100% recirculation and the air conditioner controls set to the desired set points and dead bands.
2. The three loggers were connected to the synchronizing cable and co-located in the middle of the tunnel. By adjusting the clock, the loggers were all synchronized to run from a 1 Hz signal generated by the master logger at the west site.
3. The three loggers were started simultaneously and then moved to their respective sites and connected to the sensors. At each site, a meter check was made to establish that each channel reading was within range.
4. The ventilation damper was set either for 100% fresh air or for 100% recirculation.

Data Processing

Data were recorded at either a 10 s or 60 s sample interval. The loggers averaged the reading over the sample interval. The shorter sample interval was used for experiments of circa 18-hour duration and the longer sample interval was used for experiments of circa 4.5-day duration. The 10 s sample interval is close to the response time of the humidity and anemometer sensors used. The longer sample interval gives a worst-case sampling interval that is approximately 4% of the on/off heating cycle time typically encountered in these experiments.

Unexpected occasional negative values occurred on all four of the stand of anemometers. No cause was detected for this anomaly, which could be mutual interference. Negative values were replaced by an interpolated value using adjacent positive values.

RESULTS

To facilitate a mixing performance comparison in different dimensions, a summary of the results is presented in two separate tables. Table 2 deals with the vertical dimension, and Table 3 deals with the longitudinal dimension. Both tables are formed as two rows; the top row presents results for the single-duct air distribution system, and the bottom row presents results for the boost duct air distribution system. Both tables are also formed as two major columns; the left major column presents results for air temperature, and the right major column presents results for air humidity.

For an overall comparison of the two systems, spatial homogeneity was evaluated in the form of a mean air temperature or humidity absolute difference. In Table 2 the difference was measured between the duct (D) and floor (F) levels.

TABLE 2
Vertical (Duct to Floor) Mean Air Temperature and Humidity Differences Measured at Three Sites in a Mushroom Tunnel

	Air Temperature Difference: Duct-Floor, °C				Air Humidity Difference: Duct-Floor, %RH			
	West (W)	Middle (M)	East (E)	W/M/E Mean	West (W)	Middle (M)	East (E)	W/M/E Mean
Single Duct Air Distribution	1.84	2.40	2.42	**2.22**	3.97	7.67	3.38	**5.00**
Boost Duct Air Distribution	0.16	0.28	0.22	**0.22**	0.49	0.87	2.28	**1.21**

TABLE 3
Longitudinal Mean Air Temperature Differences Measured at Four Levels and Mean Air Humidity Differences Measured at Two Levels in a Mushroom Tunnel

	Air Temperature Difference, °C					Air Humidity Difference, %RH		
	Duct (D)	Upper (U)	Lower (L)	Floor (F)	D/U/L/F Mean	Duct (D)	Floor (F)	D/F Mean
Single Duct Air Distribution	0.26	0.45	0.40	0.46	**0.39**	1.13	2.82	**1.96**
Boost Duct Air Distribution	0.24	0.43	0.46	0.43	**0.39**	0.69	2.33	**1.51**

In Table 3 the difference was calculated as the mean of the absolute difference between all three locations, i.e., east-middle, middle-west, and west-east, measured at each level, i.e., duct (D), upper air (U), lower air (L), or floor (F).

A mean of the results obtained, i.e., for all of the runs for full fresh air and for full recirculation, is presented for the appropriate measurement location. To give a single figure of merit for overall mixing performance, a mean of these results is also presented (in bold text).

From Tables 2 and 3, it can be seen that there was much lower vertical variance in air temperature and humidity for the boost duct system compared to the single-duct system. In the longitudinal dimension, no significant difference in air temperature or humidity was apparent for either system. The lower vertical variance in the boost duct system was indicative of its superior mixing performance and the absence of stratification. This variance may be more visible in a graphical comparison, which is provided in Figures 5 and 6.

Figure 4 shows a "snapshot" from the middle experimental location during a summary experimental run. The figure is divided in half to demonstrate a "before and after" scenario. In the left half of Figure 4, air distribution was through a single-duct system. In the right half of Figure 4, the boost duct system has come into play. The lower trace in Figure 4 was the airflow at floor level; note that airspeed can drop off (collapse), from around 0.25 m/s to around 0.05 m/s, in the single-duct system. This was not observed when the boost duct came into play.

The middle trace in Figure 4 was air temperature at floor level, and the top trace was air temperature at duct level. The following was noted for the single-duct system, i.e., the left hand part of Figure 4:

- During a period when the heater was on, indicated by a rise in duct level air temperature, there was a divergence of duct and floor level temperatures.
- Due to change in the thermal buoyancy of the delivered air, air stratification began and there was a drop in the floor level airspeed, i.e., this was the start of the stratification effect.

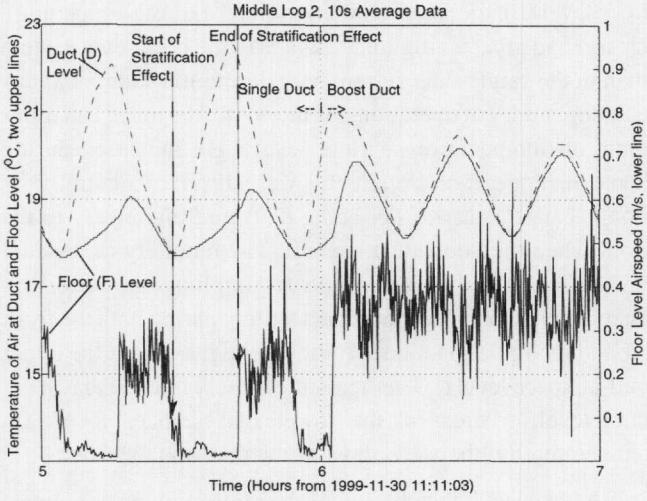

Figure 4 *Floor (F) level airspeed measurement at middle sensor site, 100% fresh air, 30 November 1999, and air temperature measurements at duct (D) and floor (F) airspace levels for both single and boost air distribution systems.*

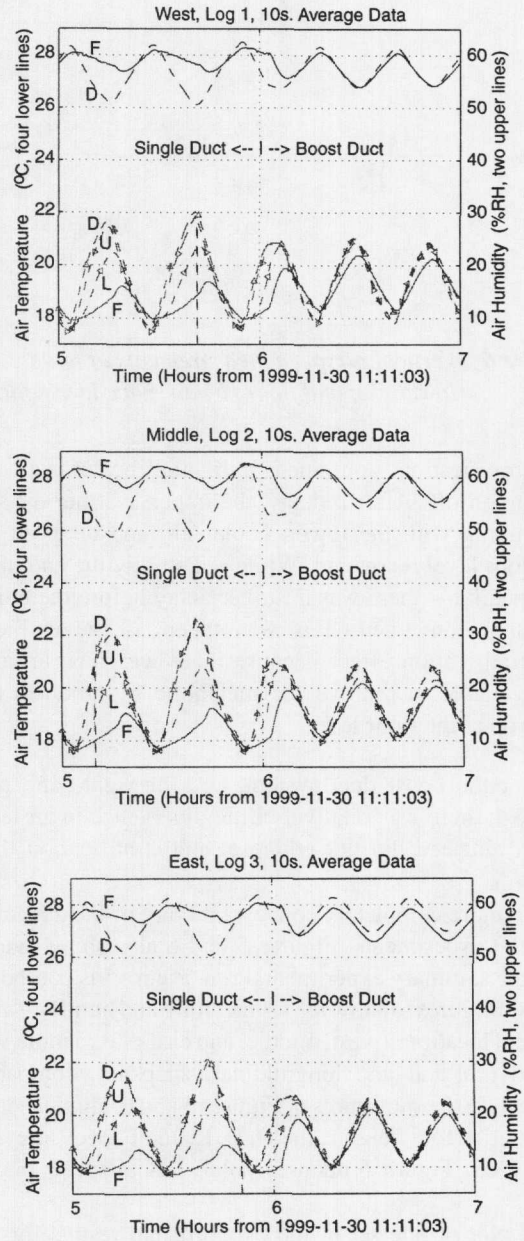

Figure 5 *Vertical temperature and humidity measurements for west, middle, and east sensor sites, 100% fresh air, 30 November 1999, at duct (D), upper (U), lower (L), and floor (F) airspace levels for both single and boost air distribution systems.*

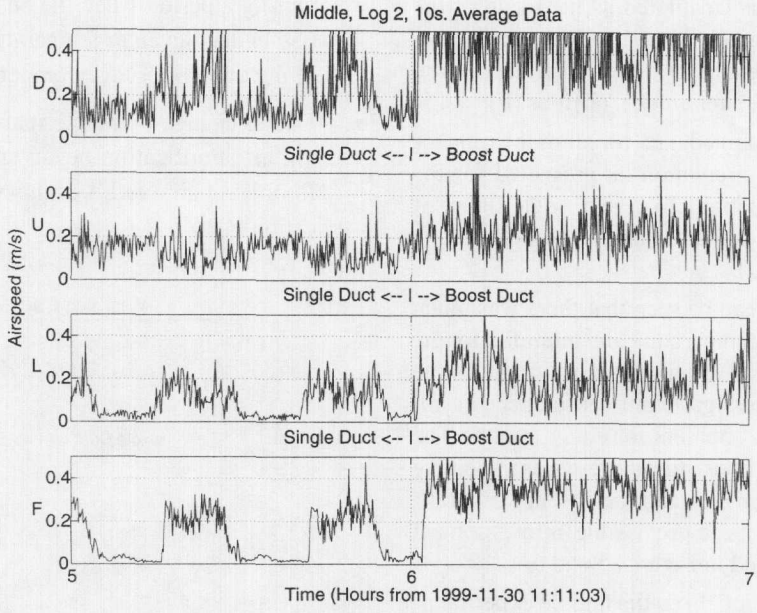

Figure 6 *Vertical airspeed measurements at middle sensor site, 100% fresh air, 30 November 1999, at duct (D), upper (U), lower (L), and floor (F) airspace levels for both single and boost air distribution systems.*

- Stratification continued until the heater valve was turned off. After a delay, the upper, warmer air started mixing with the lower, cooler air, and airspeed at the floor level recovered. While not strictly the end of stratification—there was a further delay before the temperatures converged—this was taken as the end of the stratification effect because there was now an airflow available to remove the metabolic by-products of the crop at the floor level.

For the boost duct system, i.e., the right-hand part of Figure 4, there was relatively little divergence in air temperatures, airspeed did not collapse, and stratification did not occur.

To more completely convey a picture of the data elicited from the experiments, Figures 5 and 6 also show snapshots from the summary experimental run. Figure 5 is composed of three subfigures to show the temperature and humidity at three different locations (west, middle, and east), i.e., a more widely framed (vertical and longitudinal) snapshot, compared to Figure 4. In the subfigures of Figures 5 and 6, climatic data are presented at four heights, the D, U, L, and F levels previously introduced. Figure 6 focuses solely on airspeed measurements.

A plot of one set of the experimental results for 100% fresh air is shown in Figure 5, i.e., in a west to east direction through the tunnel. As in Figure 4, the boost duct was not powered until approximately halfway through all of Figure 5, i.e., the left half of each subfigure was a single-duct system and the right half was a boost duct system. Note that the vertical spikes visible in Figure 5 show the known logger storage fault referred to previously.

Vertical/Longitudinal Comparison

As shown in the left-hand side of all of Figure 5, the temperature at the duct level (D) had swings of greater amplitude in the single-duct system than in the boost duct system both during fresh air and recirculation modes of operation. This resulted from air stratification; because heat was not being delivered effectively to the floor level, the upper air was receiving more heat during times of air stratification. At the floor level (F), the situation was reversed, i.e., the temperature clearly had greater amplitude swings in the boost duct system than in the single-duct system both during fresh air and recirculation modes of operation. Furthermore, the mean and minimum air temperatures at floor level were increased during boost duct operation. Again, this was a result of air stratification because heat was not being delivered effectively to the floor when the boost duct was off. The humidity at the duct level (D) also had swings of greater amplitude in the single-duct system than in the boost duct system during both the fresh air and recirculation modes for the same reason. At the upper mid-airspace level (U), temperature closely tracked that at the duct level, whereas at the lower mid-airspace level (L), temperature fell between those at the duct and the floor.

As expected, the phasing of the upper and lower temperatures and humidities was such that the upper air led the lower air for both single and boost duct systems. For the boost duct system, this was a result of the transit time from duct exit to floor level via the tunnel wall. For the single-duct system, it was a result of this combined with the air stratification discussed previously.

As shown in Table 3 and Figure 5, it can be seen that there was little variation in either air temperature or humidity in the longitudinal direction for either system at any level.

Airspeed

Corresponding airspeed measurements to Figure 5 (middle) are shown in Figure 6, again with single-duct measurements shown in the left half of the figure and boost duct measurements shown in the right half of the figure. Due to the high turbulence intensity of the airflow, it may appear that the airspeeds shown in Figure 6 are of a random nature. Note the influence air stratification had on floor level (F) airspeed in the single-duct system when speed dropped from a nominal 0.25 m/s (0.82 ft/s) to about 0.05 m/s (0.16 ft/s). This occurs three times in Figure 6 and was also visible at the lower mid-airspace (L) level. Also note the absence of this artifact in the boost duct system at the same levels, operating in the same thermal regime.

The data indicated that the boost duct system increased mean airspeed at all levels but especially so at duct and floor level. This showed the importance of the Coanda effect (Tritton 1977) in the delivery of air to the crop surface.

DISCUSSION

While it would have been desirable to incorporate many different climate profiles in the study, this would lead to large costs. Hence, the study was limited to a "typical growth scenario."

Several studies have established stratification temperature profiles for other applications, e.g., automotive plants (Olivieri and Singh 1979) and factories (Beier and Gorton 1978); however, no comparable study that measured climate spatial variation in several dimensions in the context of a boost duct mushroom tunnel has been located by the authors. Hence, no comparison of these results with any other work was possible. As there is a relatively large tunnel population of similar design, the results from this study have wide applicability.

Air temperature was higher at floor level for boost duct operation, which shows the higher gain of this system, and this is desirable for closed loop control. The higher floor air temperature during boost duct operation was a result of the controller temperature sensor configuration, which was positioned for single-duct operation.

Archimedes Number

The results show the superior mixing performance of the boost system. The question now arises of what is a suitable variable for control of the air distribution system. From the literature examined (Randall 1975, 1978; Randall and Battams 1979; Barber and Ogilvie 1982; Bowers et al. 1986; Leonard and McQuitty 1986a, 1986b, 1987; Berckmans et al. 1993; Zhang et al. 1992, 1996; Zhang 1996), it seems appropriate to use the Archimedes number as a means of predicting jet trajectory.

The studies listed above generally apply to a horizontal isothermal free jet. The air jet under consideration in a mushroom tunnel has a path in some form of a "C" shape, is generally attached to a surface, may or may not be isothermal, is subject to variable cross-flow, i.e., toward the exhaust or recirculation vent, and the ambient air environment may or may not be stratified. The authors have been unable to locate any study that encompasses all the characteristics of such an air jet, although several studies discuss one or more of these characteristics, e.g., Timmons et al. (1980) study the attachment length of a planar jet in a rectangular enclosure and Ball and Jones (1979) consider a horizontal jet subject to vertical cross-flow.

In summary, this application differs in the following respects:

- Unusual vents, D-shaped with nonuniform spacing.
- Airflow direction, i.e., air distribution is centrally originated.
- Two merging airflows in the case of the boost duct.
- Mixing of the isothermal jet from the boost duct with the predominantly nonisothermal jet from the primary duct.
- Strong influence of the Coanda effect; no observation of jet separation from the wall and subsequent reattachment has been observed.

As the authors located no suitable contending control variable during the literature search, further study of these points is needed to determine the suitability of the Archimedes number in this application.

CONCLUSIONS

From the lower variance in air temperature and humidity for the boost duct results, it can be inferred that there is better mixing in the boost duct system, i.e., the boost duct system has better mixing performance than the single-duct system.

The airspeed measurements indicate that a boost duct system can provide sufficient momentum to enable control of the air delivery to the crop surface. During times of air stratification, the single-duct system cannot.

The increase in mean air temperature at floor level shows that during boost duct operation, heat delivery to the floor-level crop is more effective compared to the single-duct system. The data suggest that less heat is lost through the tunnel structure and more effective energy delivery is obtained with the boost duct system. No calculation of the gain in heat delivery compared to the extra cost of powering the boost fan was made, as this was not within the scope of this study.

For modeling boost duct operation, the data collected in this study would indicate that some form of a well-mixed single-tank climate model, which incorporates the delayed delivery of air from the duct, is appropriate. The data collected in this study would also indicate that some form of a coupled "tanks in series" model, with the upper air being the first tank and the lower air being the second tank, is appropriate for single-duct operation.

ACKNOWLEDGMENTS

Thanks are due to Teagasc for access to experimental facilities and the funding of this research via a Walsh Fellowship.

REFERENCES

Barber, E.M., and J.R. Ogilvie. 1982. Incomplete mixing in ventilated airspaces, part 1, Theoretical considerations. *Canadian Agricultural Engineering* 24: 25-29.

Ball, H.D., and R.L. Jones. 1979. Analysis of a horizontally projected chilled ventilation jet subject to vertical crossflow. *ASHRAE Transactions* 85(1): 323-332.

Beier, R.A., and R.L. Gorton. 1978. Thermal stratification in factories—Cooling loads and temperature profiles. *ASHRAE Transactions* 84(1): 325-339.

Berckmans, D., J.M. Randall, D. Van Thielen, and V. Goedseels. 1993. Validity of the Archimedes number in ventilating commercial livestock buildings. *Journal of Agricultural Engineering Research* 56: 239-251.

Bowers, C.G., D.H. Willits, and H.D. Bowen. 1986. Criteria for determining buoyancy effects on turbulent forced convection in an asymmetrically heated horizontal channel. *ASAE Transactions* 29: 550-555.

Cromwell, P. 1999. Accuracy of temperature calibration system, personal communication.

Etheridge, D.W., and M. Sandberg. 1996. *Building ventilation theory and measurement.* Chichester: John Wiley.

FDS (Farm Development Service). 1987. *S.151 minimum specification for polythene-clad mushroom houses.* Dublin: Department of Agriculture.

Grant, J. 1995a. The operation of heating systems in mushroom tunnels, p. 10. Confidential report to the Irish Mushroom Growers Association. Dublin: Teagasc.

Grant, J. 1995b. Air conditions in mushroom tunnels—The effects of heating and cooling systems. *Proceedings of 11th National Mushroom Conference, Dublin*: 27-36.

Grant, J. 1999. Stratification of airflow in Irish mushroom-growing tunnels. *Proceedings of 99 International Conference on Agricultural Engineering, Beijing*, III-4 to III-8.

Leonard, J.J., and J.B. McQuitty. 1986a. Archimedes number criteria for the control of cold ventilation air jets. *Canadian Agricultural Engineering* 28: 117-123.

Leonard, J.J., and J.B. McQuitty. 1986b. The use of Archimedes number in the design of ventilation systems for animal housing. *Conference on Agricultural Engineering, Canberra.*

Leonard, J.J., and J.B. McQuitty. 1987. Air mixing in a mechanically ventilated room. *Canadian Agricultural Engineering* 30: 185-189.

Martin, D., J. Ringwood, and J. Grant. 1997. Mushroom tunnel climate: Neural networks compared. *Acta Horticulturae* 456: 477-484.

Murray, F. 1995. Modelling and control of the environmental conditions in a mushroom tunnel. M.Sc. thesis, University College, Galway.

Olivieri, J.B., and T. Singh. 1979. Effect of supply and return outlet location on stratification. *ASHRAE Transactions* 85(1): 333-342.

Randall, J. M. 1975. The prediction of airflow patterns in livestock buildings. *Journal of Agricultural Engineering Research* 20: 199-215.

Randall, J.M. 1978. The study of internal air flows and the design of ventilation systems for livestock buildings. Ph.D. dissertation, University of Reading.

Randall, J.M., and V.A. Battams. 1979. Stability criteria for airflow patterns in livestock buildings. *Journal of Agricultural Engineering Research* 24: 361-374.

Timmons, M.B., L.D. Albright, R.B. Furry, and K.E. Torrance. 1980. Experimental and numerical study of air movement in slot-ventilated enclosures. *ASHRAE Transactions* 86 (1): 221-240.

Tritton, D.J. 1977. *Physical fluid dynamics*, p. 284. Wokingham: Van Nostrand.

Wang, S., T. Boulard, and R. Haxaire. 1999. Experimental and numerical studies of airflow, temperature and humidity distributions in a greenhouse tunnel. *Proceedings of 99 International Conference on Agricultural Engineering, Beijing:* III-34 to III-38.

Zhang, G., S. Morsing, and J.S. Strom. 1992. Design principle and control strategy for an automatically controlled hybrid ventilation system. *Proceedings of AgEng92*: 182-183.

Zhang, G. 1996. Airflow pattern control in livestock buildings. *Acta Horticulturae* 406: 373-382.

Zhang, G., S. Morsing, and J.S. Strom. 1996. Modeling jet drop distances for control of a non-isothermal, flap-adjusted ventilation jet. *ASAE Transactions* 39: 1421-1431.